

Two-dimensional colloidal crystals formed by thermophoresis and convection

Stefan Duhr and Dieter Braun^{a)}

Dissipative Biosystems Lab, Applied Physics, Ludwig Maximilians Universität München, Amalienstr. 54, 80799 München, Germany

(Received 29 November 2004; accepted 3 February 2005; published online 24 March 2005)

Temperature gradients can trap micrometer-sized particles into two-dimensional crystals. We form colloidal crystals from otherwise repellent $2\ \mu\text{m}$ polystyrene beads in diverse thermal convection settings. Our experiments indicate that the accumulation is driven by particle thermophoresis. Particles move along the temperature gradient and are pushed out of the warm liquid to a cold wall. We find reduced accumulation for decreased surface temperature gradients and enhanced salt concentrations. Moreover, thermophoretic fluid dynamics calculations predict flat accumulation profiles with 10^7 -fold enhanced concentrations that are consistent with our experiments. The accumulated crystals could be used as molecular sieves for microfluidic biotechnological applications. A natural environment for similar accumulations are pores of rock near hydrothermal vents. © 2005 American Institute of Physics. [DOI: 10.1063/1.1888036]

We show how the combination of thermodiffusion and convection in a solution of polystyrene beads leads to the accumulation of a two-dimensional crystal at the cooling surface in a convective flow. This finding confirms the strong DNA accumulation found previously in a similar convection setting.¹ Here, however, the tendency to accumulate is so strong that particles are pushed out of the diluted solution into a crystal.

Thermophoresis,²⁻⁶ the movement of particles along temperature gradients, is an interfacial force which in liquids still lacks detailed understanding.⁷⁻¹¹ It can be used to separate beads¹²⁻¹⁴ and measure diffusion constants.¹⁵ The combination of convection and thermophoresis to accumulate molecules has a long history in elongated thermogravitational columns.¹⁶

Formation of colloidal crystals¹⁷⁻²² out of diluted solutions is of interest for molecular sieves, photonic crystals,²³ and chemical sensing.²⁴ Two-dimensional crystals can be used to explore statistical physics of defects.^{25,26} Ways to efficiently accumulate molecules and particles out of solution are of great interest to enhance the sensitivity of diffusion limited surface biosensors. Moreover, the forces which drive colloidal crystals might be used to enhance the crystallization of proteins. Notably, the experimental temperature gradients used in our system are compatible with natural conditions in pores of rock around hydrothermal vents.²⁷⁻³⁰ Thermophoretic trapping experiments have been performed in chambers of $500\ \mu\text{m}$ in height and $6\ \text{mm}$ in diameter (Fig. 1). On top, the chamber was sealed off by a cover glass slide (Roth No. 0657, $170\ \mu\text{m}$ thickness). The sidewalls were formed by a silicon sheet of $500\ \mu\text{m}$ thickness (McMaster, New York) while the bottom was sealed by default with a $1\ \text{mm}$ sapphire window (Edmund Optics), but for some experimental setups polymethyl siloxane (PDMS, Sylgard 184, Dow Corning) or glass (No. 0656, Roth Laborbedarf) was used. The water of the chamber was heated from below with an infrared laser (FOL1405RTV-317, Furukawa, Japan) with

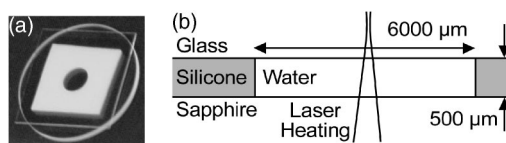


FIG. 1. Chamber. (a) Photograph of the convection chamber. (b) Liquid is filled between sapphire and glass, separated by $500\text{-}\mu\text{m}$ -thick silicone spacer with an open diameter of $6\ \text{mm}$. The center is heated by an infrared laser, inducing a toroidal convection flow.

a power of $100\ \text{mW}$. The lateral position of the laser focus could be moved by the use of two galvo-mirrors (6200-XY scanners with driver 67120, Cambridge Technologies) to form complex heating geometries. The laser beam was focused with a numerical aperture of 0.14 using a Mitutoyo near infrared-corrected $5\times$ objective. The focus plane was placed $1000\ \mu\text{m}$ above the top of the chamber to make heat-

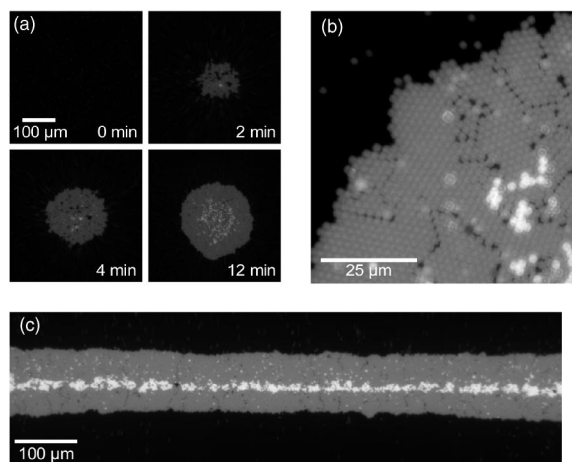


FIG. 2. Generation of two-dimensional colloidal crystal from thermophoresis and convection. (a,b) The chamber contains $2\ \mu\text{m}$ polystyrene beads at low concentration. It is heated in the center by infrared absorption. Within $12\ \text{min}$, a two-dimensional colloidal crystal forms against the 5000 -fold lower bead concentration in the liquid. (c) Heating along a line leads to the formation of an elongated crystal.

^{a)} Author to whom correspondence should be addressed; electronic mail: dieter.braun@physik.lmu.de

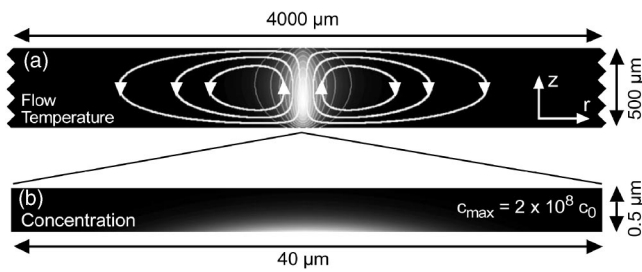


FIG. 3. Theory predicts strong and flat accumulation. (a) Heat transfer, bead diffusion, thermophoresis and Navier–Stokes flow are simulated in cylinder coordinates. We show the temperature profile and selected flow lines in a vertical cross section. (b) Predicted particle concentration reaches 2×10^8 times the bulk concentration in a very flat geometry at the lower chamber wall.

ing less focused. Due to a 6 mm $1/e^2$ -diameter-Gaussian beam in front of the objective, we heat with a 2.8° opening angle in water.

For thermophoretic trapping, 1 and 2 μm fluorescently labeled polystyrene beads were used (2% solid, F-8823, F-8827, molecular probes) and diluted 1:500 and 1:100 in 0.1 mM Tris-HCl at pH 7.8, respectively. The lower chamber wall was imaged with a $10\times$ or $32\times$ objective using a fluorescent microscope (AxioTech Vario, Zeiss). Fluorescence was excited by a high-power LED (LXHL-LX5C, Luxeon) at a driving current of 35 mA with an ILX lightwave current source (ILX 3565). A charge coupled device camera (670KS, SensiCam QE, PCO, Kehlheim) was used to take pictures of the illuminated beads with a typical frame rate of 0.03 Hz (exposure 5 s delay, 25 s).

Figures 2(a) and 2(b) show the aggregation of a crystal within 12 min of laser heating. The thermophoretic trapping chamber is filled with 14 μl of diluted 2 μm polystyrene beads (45 000 spheres per μl). Laser heating immediately induces a toroidal convection, taking the beads along with the flow. After less than 12 min, a circular monolayer of fluorescently labeled beads is formed on the bottom sapphire chamber wall [Figs. 2(a) and 2(b)]. It has a maximum diameter of about 200 μm. The bead accumulation is limited only by closest crystal packing, leading to a 5000-fold increased concentration in the crystal as compared to the solution.

Two factors create the colloidal crystal. At the bottom of the chamber, convection transports the particles below the heated center. Nonslip boundary conditions force a slow flow near the chamber walls. Since sedimentation is negligible,

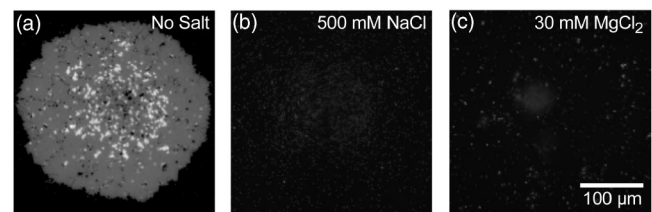


FIG. 4. No accumulation at high salt concentrations. (a-c) No accumulation is found for more than 500 mM NaCl or 30 mM MgCl₂. Thermophoresis vanishes at such high salt concentrations.

convection does not concentrate the particles. Accumulation is induced from a strong temperature gradient in z direction. Thermophoresis makes the particles follow the heat transport out of the chamber and pushes them to the lower chamber wall. The same effect is not seen at the top of the chamber since convection yields a divergent flow there.

Figure 2(c) shows how spreading the laser focus along a line leads to elongated accumulation of beads. The line was scanned by mirrors along 1.4 mm with 250 Hz and 160 mW laser power. The resulting linear accumulation demonstrates that radially convergent flow is not necessary to form a colloidal crystal.

A finite element calculation confirms the thermophoretic accumulation (Fig. 3). As described previously,³¹ the numerical program FEMLAB allows parallel solving of Navier–Stokes flow, heat conductivity, diffusion, and thermophoresis. The convection takes place on the 1000 μm scale and the accumulation on the μm scale. Thus a highly adapted grid was necessary for the simulation. The diffusion constant for 2 μm spheres is $D=0.2 \mu\text{m}^2/\text{s}$ according to the Stokes–Einstein relation $D=(k_B T)/(6\pi\eta r)$. As thermal diffusion coefficient we used $D_T=3 \mu\text{m}^2/(\text{s K})$ based on preliminary thermophoresis measurements using single particle tracking. No fitting parameters were used.

The simulation shows that the center of the chamber is heated to 62 °C and leads to a maximum convection speed of 580 μm/s. Temperature gradients in the central accumulation region are small in radial direction ($\partial_r T=10^3 \text{ K/m}$) and strong vertically ($\partial_z T=8 \times 10^5 \text{ K/m}$). Therefore the temperature gradient pushes the particles downwards with a drift velocity of $D_T \partial_z T=2.5 \mu\text{m/s}$.

The simulation predicts very strong thermophoretic accumulation. We expect a 2×10^8 -fold enhanced concentration near the lower chamber wall. The concentration falls off

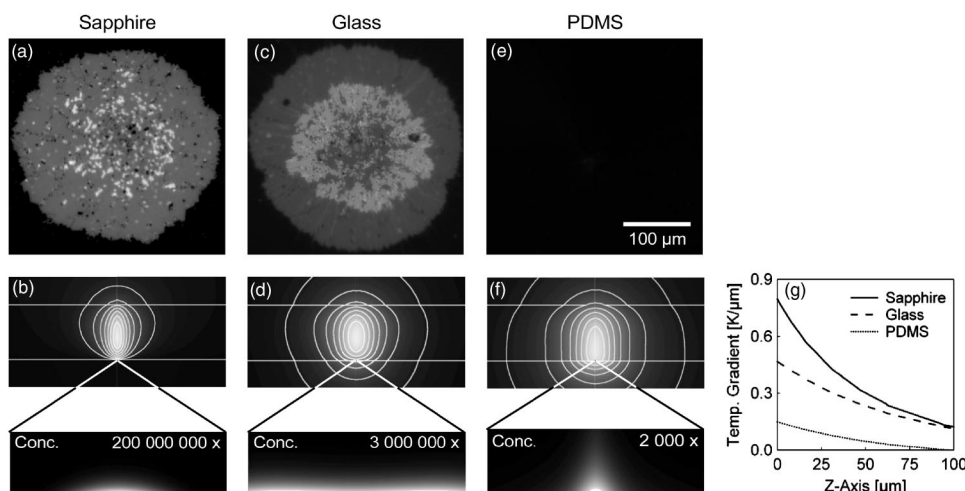


FIG. 5. Accumulation on different substrates. (a,c,e) The temperature gradient in z direction was modified by changing the substrate material from sapphire (a) to glass (c) and PDMS (e). The heat conductivity is decreased by more than two orders of magnitude. (b,d,f) Simulations show a strong change in the vertical temperature gradient. Concentration drops over five orders of magnitude from 2×10^8 over 3×10^6 down to 2×10^3 as we go from sapphire over glass to PDMS. (g) The central temperature gradients in z direction as obtained by the simulation.

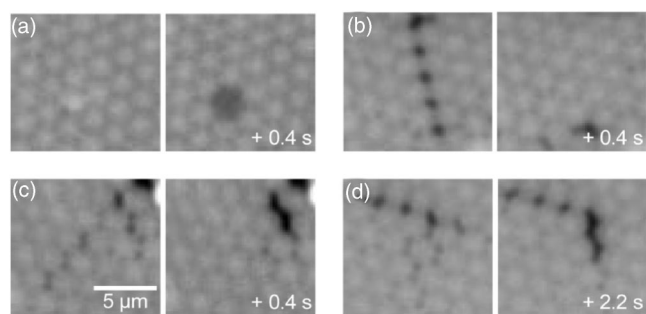


FIG. 6. Crystal defect dynamics. The accumulated crystal shows diverse defects with a fast and a rich dynamics. We show some examples. (a) A point defect builds up by the removal of a bead within 0.4 s. (b) A fault line closes within 0.4 s. (c) A fault line closes by opening a neighboring one. (d) Compression of unordered particles to a crystal.

to half its value within a diameter of $20 \mu\text{m}$ and a height of $0.5 \mu\text{m}$. The height is fourfold smaller than the accumulated particles. The particles therefore effectively average the simulated concentration profile. In our experiments, the accumulation is 5000-fold since stronger accumulation is hindered sterically by the crystal.

Figure 4 shows how adding salt quenches the accumulation. We added 500 mM NaCl or 30 mM MgCl_2 where it is known that thermophoresis is quenched.^{1,9} Although the particles have an enhanced tendency to stick to the surface under these conditions, accumulation vanishes. At high salt concentrations, convective flow alone does not lead to accumulation.

The temperature gradient near the lower wall is essential as seen in Fig. 5. Crystal formation vanishes if the heat conductivity of the lower substrate is reduced. This is done by replacing the lower chamber wall from sapphire [Fig. 5(a), heat conductivity $\lambda=34 \text{ Wm}^{-1}\text{K}^{-1}$] to glass [Fig. 5(c), $\lambda=1.4 \text{ Wm}^{-1}\text{K}^{-1}$] and PDMS [Fig. 5(e), $\lambda=0.18 \text{ Wm}^{-1}\text{K}^{-1}$]. Simulations of different bottom materials confirm this as the concentration drops over many orders of magnitude from 2×10^8 over 3×10^6 down to 2×10^3 (Figs. 5(b)–5(f)). This high sensitivity confirms the dominating role of the vertical temperature gradient [Fig. 5(g)].

Crystal defect dynamics can be observed as shown in Fig. 6. Point defects can appear by bead removal within 0.4 s [Fig. 6(a)], and line defects can rearrange within the same time span [Fig. 6(b)]. More complex rearrangements can also be seen [Figs. 6(c) and 6(d)]. These images demonstrate that the accumulated crystals can be used to simulate basic defect dynamics.

At incubation times longer than 12 min, up to three layers of beads accumulate to reach a steady state after 60 min [Fig. 7(a)]. The layers were observed in an intensity histogram as peaks [Fig. 7(b)]. A fourth layer does not nucleate into crystals, but consists only of loosely attached beads.

Our experiments demonstrate that micrometer-sized particles can be strongly accumulated by a combination of thermophoresis and convection. The mechanism has applications in microfiltration, particle accumulation, and molecular detection on surfaces. We expect that the demonstrated strong

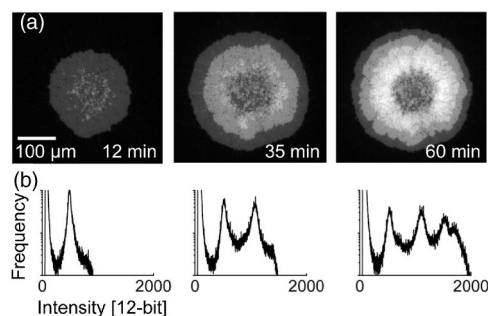


FIG. 7. Generation of multilayered crystal over time. Up to three crystal layers are formed within 60 min as seen as peaks in the intensity histograms.

accumulation of particles can lead to a co-accumulation of molecules.

The authors thank Roberto Cerbino for discussions, the Deutsche Forschungsgemeinschaft (DFG) for funding through the Emmy Noether Program II, and Hermann Gaub for hosting our lab.

- ¹D. Braun and A. Libchaber, *Phys. Rev. Lett.* **89**, 188103 (2002).
- ²C. Soret, *Arch. Geneve* **3**, 48 (1879).
- ³C. Ludwig, *Sitzber. Akad. Wiss. Wien, Math.-Naturw. Kl.* **20**, 539 (1856).
- ⁴J. C. Maxwell, *J.C. Collected Papers II* (Cambridge University Press, Cambridge), 1890, pp. 681–712
- ⁵P. S. Epstein, *Z. Phys.* **54**, 537 (1929).
- ⁶S. R. de Groot and P. Mazur, *Non-equilibrium Thermodynamics* (North-Holland, Amsterdam, 1969).
- ⁷W. Köhler and P. Rossmann, *J. Phys. Chem.* **99**, 5838 (1995).
- ⁸C. Debuschewitz and W. Köhler, *Phys. Rev. Lett.* **87**, 055901 (2001).
- ⁹R. Piazza and A. Guarino, *Phys. Rev. Lett.* **88**, 208302 (2002).
- ¹⁰S. Iacopini and R. Piazza, *Europhys. Lett.* **63**, 247253 (2003).
- ¹¹R. Rusconi, L. Isa, and R. Piazza, *J. Opt. Soc. Am. B* **21**, 605 (2004).
- ¹²M. E. Schimpf and J. C. Giddings, *J. Polym. Sci., Part B: Polym. Phys.* **28**, 2673 (1990).
- ¹³B. K. Gale, K. D. Caldwell, and A. B. Frazier, *IEEE Trans. Biomed. Eng.* **45**, 1459 (1998).
- ¹⁴T. L. Edwards, B. K. Gale, and A. B. Frazier, *Anal. Chem.* **74**, 1211 (2002).
- ¹⁵M. Giglio and A. Vendramini, *Phys. Rev. Lett.* **38**, 26 (1977).
- ¹⁶K. Clusius and G. Dickel, *Z. Phys. Chem. Abt. B* **44**, 397 (1939).
- ¹⁷I. M. Krieger and F. M. O'Neill, *J. Am. Chem. Soc.* **90**, 3114 (1968).
- ¹⁸N. A. Clark, A. J. Hurd, and B. J. Ackerson, *Nature (London)* **281**, 57 (1979).
- ¹⁹R. J. Carlson and S. A. Asher, *Appl. Spectrosc.* **38**, 297 (1984).
- ²⁰D. J. W. Aastuen, N. A. Clark, L. K. Cotter, and B. J. Ackerson, *Phys. Rev. Lett.* **57**, 1733 (1986).
- ²¹E. A. Kamenetzky, L. G. Magliocco, and H. P. Panzer, *Science* **263**, 207 (1994).
- ²²P. Schall, I. Cohen, D. A. Weitz, and F. Spaepen, *Science* **305**, 1944 (2004).
- ²³J. E. G. J. Wijnhoven and W. L. Vos, *Science* **281**, 802 (1998).
- ²⁴J. H. Holtz and S. A. Asher, *Nature (London)* **389**, 829 (1997).
- ²⁵C. A. Murray, in *Bond-Oriented Order in Condensed Matter Systems*, edited by K. J. Strandburg (Springer, New York, 1992).
- ²⁶K. Zahn, R. Lenke, and G. Maret, *Phys. Rev. Lett.* **82**, 2721 (1991).
- ²⁷D. Braun and A. Libchaber, *Physical Biology* **1**, 1 (2004).
- ²⁸M. J. Russell, A. J. Hall, A. G. Cairns-Smith, and P. S. Braterman, *Nature (London)* **336**, 117 (1988).
- ²⁹N. G. Hohn (editor), *Origins Life Evol. Biosphere* **22**, 1 (1992).
- ³⁰C. L. Van Dover, *The Ecology of Deep-Sea Hydrothermal Vents* (Princeton University Press, Princeton, NJ, 2000).
- ³¹S. Duhr, S. Arduini, and D. Braun, *Eur. Phys. J. E* **15**, 277 (2004).